Research Article | Vol. 26, No. 18 | 3 Sep 2018 | OPTICS EXPRESS 23278
Optics EXPRESS

Two-dimensional stitching interferometry based on tilt measurement

LEI HUANG,[1,*] MOURAD IDIR,[1] CHAO ZUO,[2] TIANYI WANG,[1] KASHMIRA TAYABALY,[1] AND ERICH LIPPMANN[3]

[1]National Synchrotron Light Source II, Brookhaven National Laboratory, Upton, NY 11973, USA
[2]School of Electronic and Optical Engineering, Nanjing University of Science and Technology, No. 200 Xiaolingwei Street, Nanjing, Jiangsu Province 210094, China
[3]Kornacker 4, Schaufling, Freistaat Bayern 94571, Germany
[*]huanglei0114@gmail.com

Abstract: In this paper, a two-dimensional stitching interferometry system using two tiltmeters is proposed. During the scanning and the measurement, one tiltmeter stays with the interferometer and the other one is attached to the translation stage where the surface under test is placed. The differences of the *x*- and *y*-tilt readings between these two tiltmeters are recorded as the relative tilt between interferometer and surface under test. The relative tilt in both *x*- and *y*-directions are used to correct the surface tip/tilt of each subset, and then the piston is adjusted to get the final stitching surface map. As an example, a stitching result of a 125mm-long mirror surface is presented. The repeatability of our current stitching system is about 1.48 nm RMS. The stitching result is compared to the result of a one-dimensional angular-measurement-based stitching method to discuss the merits and limitation of the proposed method.

1. Introduction

The sub-aperture stitching technique is one of the most flexible and practical solutions generally used in optical surface metrology [1–3] to resolve the problem of measuring a large surface with a limited single field of view, or measuring a large curvature range with a limited measuring range. With the scanning mechanism and stitching procedure, it enables the possibility of maintaining the lateral spatial resolution of a single subset while measuring the full surface. The stitching technique has been applied in optical interferometry metrology to overcome the high cost and technical challenges of making an accurate interferometric instrument with a large field of view. The stitching interferometry is one of the high-precision optical surface metrology techniques that has been used in various applications [4–6], in which the stitching methods were mainly based on software stitching algorithms to minimize the surface difference in overlapping regions [7].

To avoid the influence on the stitching results from the retrace error from interferometers [8, 9], which will affect the accuracy and precision of the tip/tilt estimations when minimizing the overlapping surface difference, another category of stitching interferometry is assisted with additional accessorial measurement information, such as the global profile with low spatial resolution or the angular measurement, by introducing extra trustable measurement devices. The micro-stitching interferometry [10] is assisted with a Fizeau interferometer measuring the global profile. The relative angle determinable stitching interferometry [10–15] measures the relative tilt of the motion with a flat mirror placed aside the surface under test. The angular measurement stitching techniques [16–18] use other angular measurement devices to measure the tilt of the stage at each scanning step to help the stitching process. Recently, electronic tiltmeters have been used to determine the tilt with 0.01 arcsec in flatness metrology [19].

In this work, we present a two-dimensional (2D) Tilt-measurement-based Stitching Interferometry (TSI), an interferometry stitching technique coupled with the tilt measurement using two tiltmeters. One tiltmeter stays with the optical sensor (for instance, an interferometer) and the

#338832 https://doi.org/10.1364/OE.26.023278
Journal © 2018 Received 16 Jul 2018; revised 12 Aug 2018; accepted 14 Aug 2018; published 27 Aug 2018

Optics EXPRESS

other one is fixed with the Surface Under Test (SUT) to track the tilts during the scanning motion. Both x-tilt and y-tilt are determined by the differential signals of the two tiltmeters to complete the 2D stitching of the measured height subsets.

2. Basic principle of the 2D TSI

In order to stitch the individual subsets of height maps in 2D, three parameters for each subset, *i.e.* piston p, x-tilt t_x, and y-tilt t_y need to be determined either by optimization algorithms [7] or using some additional hardware [10–12, 16–18]. In the proposed TSI, as shown in Fig. 1, S_n is the nth stitched subset and M_{n+1} is the next adjacent measured subset. The two tiltmeters measure the relative t_x and t_y between the interferometer and surface under test.

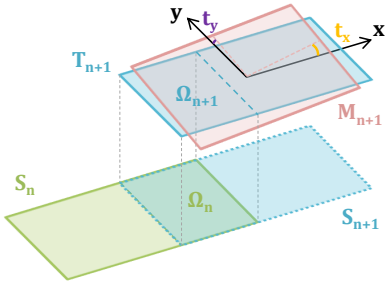

Fig. 1. The 2D stitching is fulfilled by adjusting the piston level of the neighboring subsets after the tilt correction assisted by the tilt measurement.

First, M_{n+1} is corrected with tilts in both x- and y-directions, and the tilt correction result is named as T_{n+1}.

$$T_{n+1} = M_{n+1} - t_x \cdot x - t_y \cdot y. \tag{1}$$

Second, p is estimated by calculating the average height difference between their overlapping areas Ω_n and Ω_{n+1}. Last, T_{n+1} is adjusted in terms of the piston and becomes the stitched subset S_{n+1} in Fig. 1.

$$S_{n+1} = T_{n+1} - p. \tag{2}$$

For more general cases of the 2D stitching, the subsets may have several overlaps with its neighboring pieces, therefore the least squares estimation should be applied to globally optimize the piston adjustment [7, 20].

3. Setup of the 2D TSI

The 2D TSI instrument is composed with an interferometer, a translation stage, and two tiltmeters.

As illustrated in Fig. 2, we attach the tiltmeter 1 with a tip/tilt stage on the granite table. The tiltmeter 2 with a tip/tilt stage is mounted on the translation stage where the SUT is placed. During the scanning process, the tiltmeters measure the tilts of the interferometer (tiltmeter 1) and the SUT (tiltmeter 2) in both x- and y-directions. Their relative x-tilt and y-tilt in Eq. (1) can be determined by taking the difference between the two tiltmeter signals.

In our actual experimental setup shown in Fig. 3, a Zygo New View 6300 White Light Interferometer (WLI) is used as an optical sensor to capture the local topographic maps of the mirror under test which is placed on an x-translation stage. Two tiltmeters (LGM HRTM) are utilized for x- and y-tilts acquisition.

Moreover, in order to evaluate the stitching results, an autocollimator (AC) (Möller-Wedel Optical ELCOMAT 3000) coupled with a 2-inch-wide flat mirror are added as an angular

Optics EXPRESS

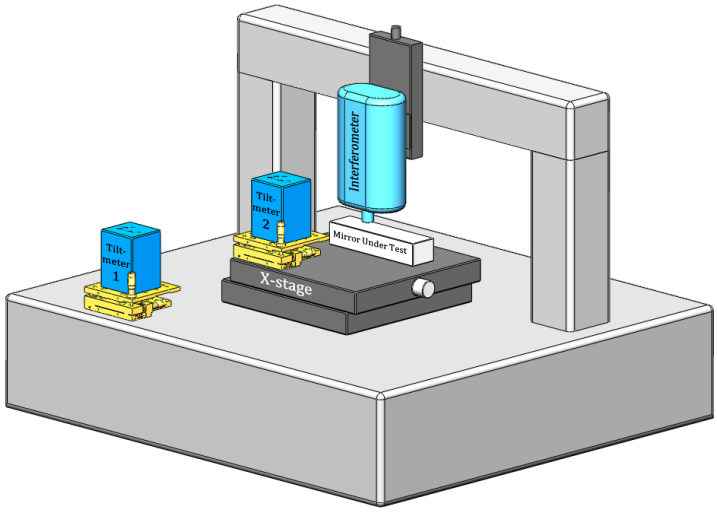

Fig. 2. The sketch of the 2D TSI system includes an interferometer which measures the height map of each subset, a translation stage, and two tiltmeters which measures the relative tilts in *x*- and *y*-directions between the interferometer and mirror under test during the scans.

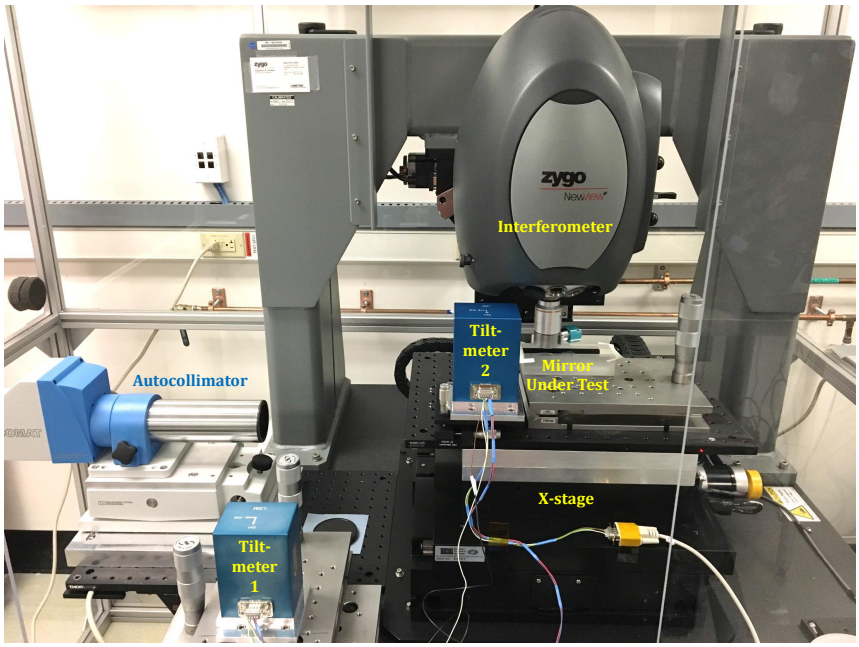

Fig. 3. The actual 2D TSI setup in the experiment includes a white light interferometer, a translation stage, and two tiltmeters. In addition, an autocollimator coupled with a reflective mirror is used to compose a 1D ASI for comparison purpose.

Optics EXPRESS

measurement device to compose a one-dimensional (1D) Angular-measurement-based Stitching Interferometer (ASI) [18] for comparison. All devices mentioned above are installed inside an enclosure to enhance the temperature stability and reduce the influence of potential air turbulence.

4. Experiment and results

Several experiments were carried out to verify the feasibility of the proposed stitching approach. During the mirror scanning, the two tiltmeters measure the tilt values of the WLI and the SUT. These two tiltmeters are synchronized by a modified serial port cable which enables the two tiltmeter to record the values at the same time when a command is sent to the serial port. The tilt measurement time is 2 seconds for each readout of the two tiltmeters in our experiment. The WLI takes a 7-averaged measurement at each scanning step.

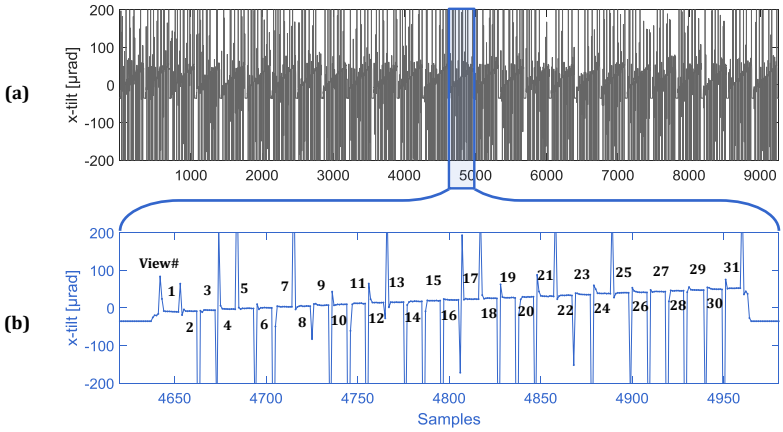

Fig. 4. Typical differential signals of x-tilt between the two tiltmeters during numbers of repeating scans (a) and typical x-tilt signals in a single scan period with 31 sub-aperture views (b).

The relative difference signals of the two tiltmeters are recorded as the final output of the tilt measurement. Figure 4(a) demonstrates some typical relative x-tilt signals in our experiment. Among these repeating scans, if we look closely into one of the scanning periods as shown in Fig. 4(b), the tilt signal is resolvable at each scanning step during the interferometer acquisition.

Figure 5 illustrates both x-tilt and y-tilt signals within one scan period, and several height maps along the scanning locations are shown Figs. 5(c)-5(g). It is worth noting that the tilts in height maps include not only the stage tilt we measured in Figs. 5(a) and 5(b), but also the tilt introduced by the mirror surface shape. The SUT used in our experiment is an elliptical cylindrical synchrotron mirror. The clear aperture of this mirror is around 125mm $\times$ 3mm. The parameters of the ideal ellipse are listed in Table 1. The 125-mm-long effective area is covered by 31 pieces subsets with a 25% overlap. It takes about 9 mins to complete one scan.

First, we compare the repeatability of the proposed TSI method with the software stitching method on our experimental data. In the software stitching method, the piston, x-tilt, and y-tilt can be estimated with a least squares plane fitting of the height difference between two WLI measured topographic data in the overlapping area. Figure 6(a) visualizes 16 repeating measurement results with the software stitching method. As a comparison, the TSI results shown in Fig. 6(b) obviously shows a more than 23% difference in terms of the peak-to-valley (PTV) values in height.

More significantly, if we take the average of the 16 scans as the reference to study the repeatability of the measurements, we can notice that the repeatability of the software stitching method [see Fig. 6(c)] is much worse than the TSI method [see Fig. 6(d)], *i.e.* 82.31 nm RMS *vs.*

Optics EXPRESS

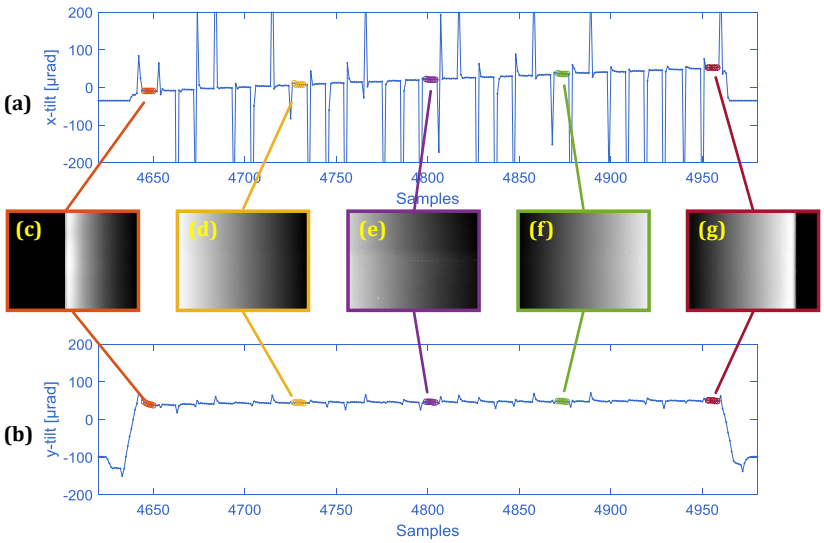

Fig. 5. Typical data from tiltmeters and WLI: The differential signals of x-tilt (a) and y-tilt (b) between the two tiltmeters in a single scan, and (c-g) five typical WLI-measured height results across the mirror under test.

Table 1. **Parameters of the target ellipse**

Parameter	Value
Source-to-mirror distance	45.170 m
Mirror-to-focus distance	331.91 mm
Grazing angle	2.8 mrad

1.43 nm RMS. The TSI measurement in our experiment achieves nanometer level repeatability. By enlarging the height discrepancies of each TSI scan as illustrated in Fig. 6(e), which shows the detailed variations and height difference of each individual scan.

As mentioned above, we also set up a 1D ASI by using an AC to further evaluate the proposed 2D TSI. While the 2D TSI is acquiring data, the 1D ASI can record the relative x-tilt data. We compare the y-tilt signals from tiltmeters and the AC as plotted in Fig. 7.

Figure 7(a) plots the x-tilt values of the 16 repeating scans by the tiltmeters and the AC. There is a vertical shift of the AC values for better visualization. For tiltmeter and AC, the repeatability of the x-tilt measurement is shown in Figs. 7(b) and 7(c), respectively. The repeatability of the tiltmeters is about 178 nrad RMS while the repeatability of the AC is about 67 nrad RMS. Obviously, the AC has higher repeatability than the tiltmeter used in our experiment.

Since the data acquisition by the AC, the tiltmeter, and the WLI are taken at the same time, they can share the same WLI data to complete their own stitching processes separately. The 2D TSI result is a 2D height map which can be visualized in 3D as shown in Fig. 8(a). However, the 1D ASI only measures a one-line profile across the SUT, so we plot one profile on the 2D TSI result to make the comparison with 1D ASI result as plotted in Fig. 8(b). They are close to each other, and for more quantitative comparison, the difference between these two profiles are plotted in Fig. 8(c). The profile discrepancy is about 80 nm PTV. The main contribution to the

Optics EXPRESS

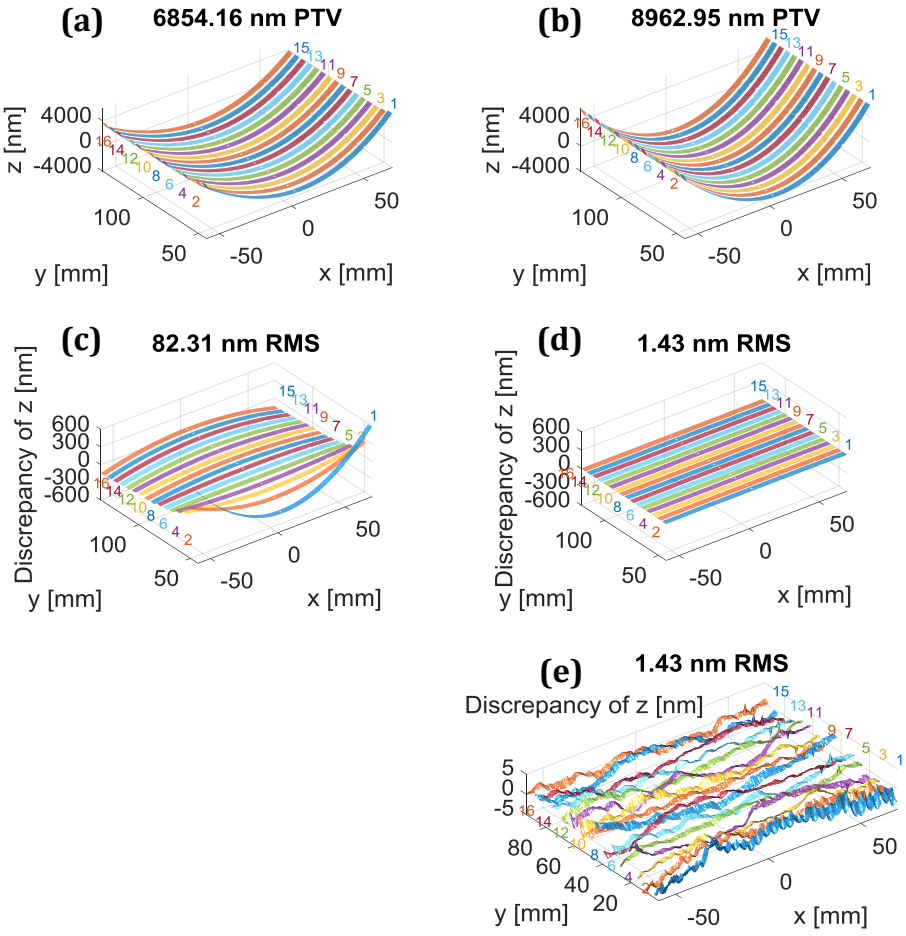

Fig. 6. Comparing to 16 repeating software stitching results (a), 16 repeating TSI stitching results (b) are much more repeatable. The stitching discrepancies by TSI (d) are much lower than those by software stitching (c). The plot (e) is an enlarged view of the same data in (d).

Optics EXPRESS

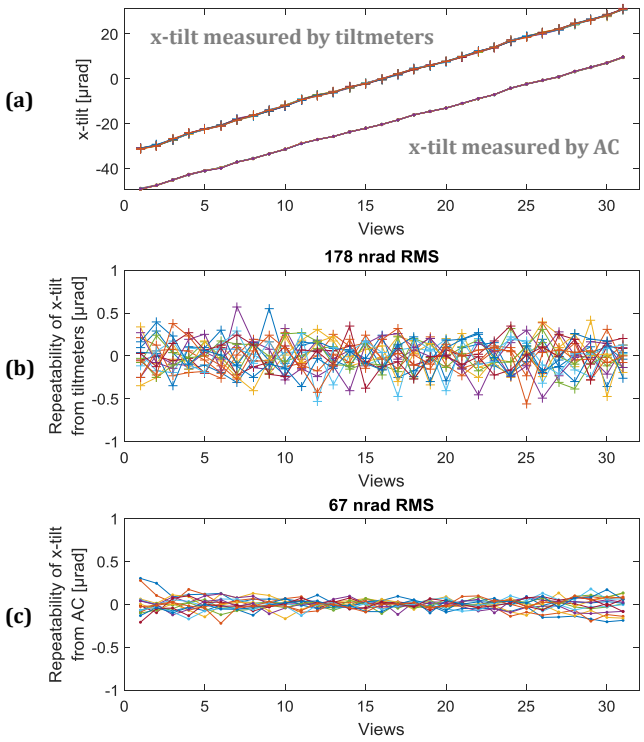

Fig. 7. Comparing the x-tilt signals measured by the tiltmeters and the AC (a), we can find the repeatability of the x-tilt measured by the tiltmeters used in our experiment (b) is worse than that of the used AC (c).

discrepancy is a power term which indicates a curvature difference.

By removing the target ellipse with the parameters shown in Table 1 from the measured profiles by TSI and ASI, their residuals are shown in Fig. 8(d). Because the center of the mirror is adjustable in the ellipse fitting, the curvature difference between the two profiles appears much less in the residual comparison. Fig. 8(e) shows the about 20 nm PTV discrepancy of the residuals from the TSI and the ASI methods.

5. Discussion

The 2D TSI has a significantly enhanced relative repeatability compared to the software stitching method and a 2D stitching capability superior to the 1D ASI. These two features highlight very promising potentials of the 2D TSI method to achieve tight 2D stitching requirements for various measurements and inspection application such as the wafer inspection.

Since the AC used in our experiment provides more repeatable x-tilt data than the tiltmeters does in the particular measuring condition [compare Figs. 7(b) and 7(c)], it is not surprising to find out the residuals resulted from ASI are more repeatable than those from TSI results [see Fig. 9]. Two reasons are concluded based on our investigation as follows.

First, the repeatability of the difference signal of the two tiltmeters is worse than the AC used in our experiment when performing measurement in a stationary scenario. This may be due to that fact that the tilt signal generated by the single tiltmeter is obviously larger than the difference signal between the two tiltmeters in our experiment environment.

Second, the tiltmeters are supposed to be used in a stationary scenario. Although we have

Optics EXPRESS

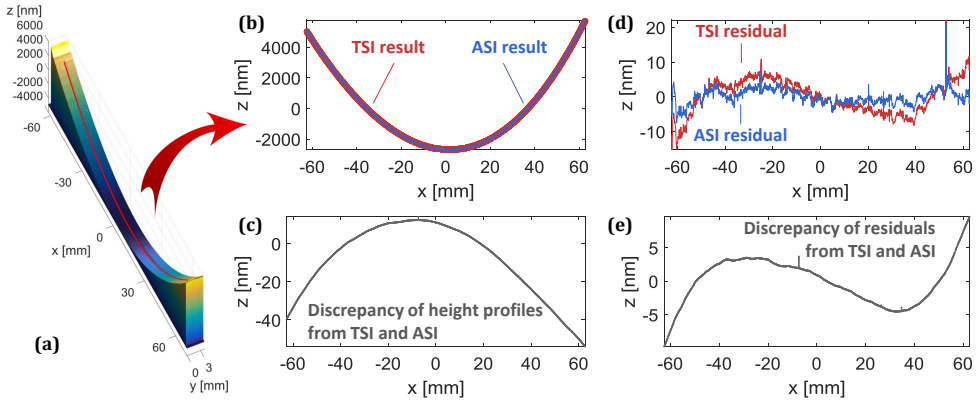

Fig. 8. The central line of the 2D TSI result (a) is compared with the 1D ASI result (b). The difference between TSI and ASI profiles is mainly a power term (c). The residuals from TSI and ASI after removing the best fit of the target ellipse (d) are compared by showing the discrepancy of their fitting residuals (e).

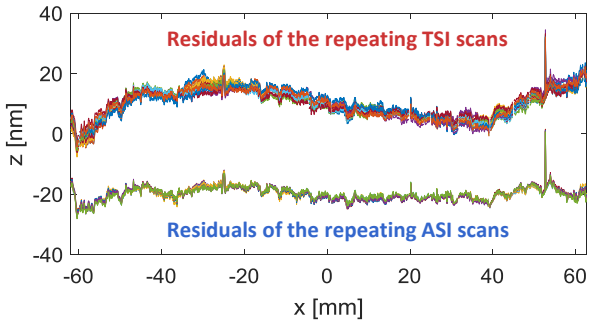

Fig. 9. The residuals of 16 repeating 2D TSI and 1D ASI scans clearly demonstrate that the repeatability of the TSI with the used tiltmeter under the measuring condition is worse than the repeatability of the ASI with the used AC, which is consistent with the repeatability of the tilt measurement results in Fig. 7.

already slowed down the stage motion, the acceleration and deceleration during the scanning could affect the readouts of the tiltmeters. The influence will be severe especially if the timing is not properly studied and tuned.

Moreover, regarding the measurement accuracy, the alignment of elements in the 2D TSI can be complicated, as the x-axis and y-axis of the two tiltmeters need to be aligned with each other, and the x-axis of tiltmeters should be aligned with the x-axis of the interferometer. The possible misalignment limits our system accuracy.

6. Conclusion

We present a 2D stitching method for stitching interferometry with the assistance of tilt measurement by using two tiltmeters. In our current setup, the repeatability of the tilt measurement from the difference signals of the tiltmeters we used is less than 200 nrad RMS. The resultant stitching height repeatability of the 2D TSI system is about 1.43 nm RMS.

Further improvements on the current system may be achieved by getting more repeatable tilt measurements, and by conducting more careful component alignment and sensor calibration of the stitching instrument.

Optics EXPRESS

Funding

Department of Energy (DOE) Office of Science (DE-SC0012704).

Acknowledgments

The authors would like to thank Dennis Kuhne from the Research & Development Group of NSLS-II for the mechanical machining. This research used resources of the National Synchrotron Light Source II, a U.S. Department of Energy (DOE) Office of Science User Facility operated for the DOE Office of Science by Brookhaven National Laboratory under Contract No. DE-SC0012704.

References

1. M. Bray, "Stitching interferometry: how and why it works," Proc. SPIE **3739**, 259–273 (1999).
2. P. Murphy, G. Forbes, J. Fleig, P. Dumas, and M. Tricard, "Stitching interferometry: a flexible solution for surface metrology," Opt. Photonics News **14**(5), 38–43 (2003).
3. M. Idir, K. Kaznatcheev, G. Dovillaire, J. Legrand, and R. Rungsawang, "A 2D high accuracy slope measuring system based on a Stitching Shack Hartmann Optical Head," Opt. Express **22**(3), 2770–2781 (2014).
4. M. Schulz, I. Weingaertner, C. Elster, and J. Gerhardt, "Low- and mid-spatial-frequency component measurement for aspheres," Proc. SPIE **5188**, 287–295 (2003).
5. Y. Wen, H. Cheng, H.-Y. Tam, and D. Zhou, "Modified stitching algorithm for annular subaperture stitching interferometry for aspheric surfaces," Appl. Opt. **52**(23), 5686–5694 (2013).
6. J. Peng, Q. Wang, X. Peng, and Y. Yu, "Stitching interferometry of high numerical aperture cylindrical optics without using a fringe-nulling routine," J. Opt. Soc. Am. A **33**(11), 1964–1972 (2015).
7. M. Otsubo, K. Okada, and J. Tsujiuchi, "Measurement of large plane surface shapes by connecting small-aperture interferograms," Opt. Eng. **33**(2), 608–613 (1994).
8. C. B. Kreischer, "Retrace error: interferometry's dark little secret," Proc. SPIE **8884**, 88840X (2013).
9. H. Yiwei, X. Hou, Q. Haiyang, and W. Song, "Retrace error reconstruction based on point characteristic function," Opt. Express **23**(22), 28216–28223 (2015).
10. K. Yamauchi, K. Yamamura, H. Mimura, Y. Sano, A. Saito, K. Ueno, K. Endo, A. Souvorov, M. Yabashi, K. Tamasaku, T. Ishikawa, and Y. Mori, "Microstitching interferometry for x-ray reflective optics," Rev. Sci. Instruments **74**(5), 2894–2898 (2003).
11. H. Mimura, H. Yumoto, S. Matsuyama, K. Yamamura, Y. Sano, K. Ueno, K. Endo, Y. Mori, M. Yabashi, K. Tamasaku, Y. Nishino, T. Ishikawa, and K. Yamauchi, "Relative angle determinable stitching interferometry for hard x-ray reflective optics," Rev. Sci. Instruments **76**(4), 045102 (2005).
12. H. Yumoto, H. Mimura, T. Kimura, S. Handa, S. Matsuyama, Y. Sano, and K. Yamauchi, "Stitching interferometric metrology for steeply curved x-ray mirrors," Surf. Interface Analysis **40**(6-7), 1023–1027 (2008).
13. T. Kimura, H. Ohashi, H. Mimura, D. Yamakawa, H. Yumoto, S. Matsuyama, T. Tsumura, H. Okada, T. Masunaga, Y. Senba, S. Goto, T. Ishikawa, and K. Yamauchi, "A stitching figure profiler of large X-ray mirrors using RADSI for subaperture data acquisition," Nucl. Instruments Methods Phys. Res. Sect. A: Accel. Spectrometers, Detect. Assoc. Equip. **616**(2), 229–232 (2010).
14. A. Vivo, B. Lantelme, R. Baker, and R. Barrett, "Stitching methods at the European Synchrotron Radiation Facility (ESRF)," Rev. Sci. Instruments **87**(5), 051908 (2016).
15. H. Yumoto, H. Mimura, S. Handa, T. Kimura, S. Matsuyama, Y. Sano, H. Ohashi, K. Yamauchi, and T. Ishikawa, "Stitching-angle measurable microscopic-interferometer: Surface-figure metrology tool for hard X-ray nanofocusing mirrors with large curvature," Nucl. Instruments Methods Phys. Res. Sect. A: Accel. Spectrometers, Detect. Assoc. Equip. **616**(2), 203–206 (2010).
16. C. Elster, I. WeingÃđrtner, and M. Schulz, "Coupled distance sensor systems for high-accuracy topography measurement: Accounting for scanning stage and systematic sensor errors," Precis. Eng. **30**(1), 32–38 (2006).
17. J. Xue, L. Huang, B. Gao, K. Kaznatcheev, and M. Idir, "One-dimensional stitching interferometry assisted by a triple-beam interferometer," Opt. Express **25**(8), 9393–9405 (2017).
18. L. Huang, J. Xue, B. Gao, and M. Idir, "One-dimensional angular-measurement-based stitching interferometry," Opt. Express **26**(8), 9882–9892 (2018).
19. G. Ehret, S. Laubach, and M. Schulz, "Flatness metrology based on small-angle deflectometric procedures with electronic tiltmeters," Proc. SPIE **10326**, 1032604 (2017).
20. L. Huang and A. K. Asundi, "Framework for gradient integration by combining radial basis functions method and least-squares method," Appl. Opt. **52**(24), 6016–6021 (2013).